3D Particle Trajectories Observed by Orthogonal Tracking Microscopy

January 22, 2009

Matthew D. McMahon, Andrew J. Berglund, Peter Carmichael, Jabez J. McClelland, and J. Alexander Liddle

Center for Nanoscale Science and Technology, National Institute of Standards and Technology, Gaithersburg, MD 20899

matthew.mcmahon@nist.gov

Keywords: orthogonal tracking microscopy, particle tracking, three-dimensional microscopy, optical microscopy, digital video microscopy, multiple vantage point microscopy

Abstract. We demonstrate high-resolution, high-speed 3D nanoparticle tracking using angled micromirrors. When angled micromirrors are introduced into the field of view of an optical microscope, reflected side-on views of a diffusing nanoparticle are projected alongside the usual direct image. The experimental design allows us to find the 3D particle trajectory using fast, centroid-based image processing, with no nonlinear computing operations. We have tracked polystyrene particles of 190 nm diameter with position measurement precision < 20 nm in 3D with 3 ms frame duration (*i.e.* at an imaging rate > 330 frames per second). Because the image processing requires only ≈ 1 ms per frame, this technique could enable real-time feedback-controlled nanoparticle assembly applications with nanometer precision.

Conventional microscopes used in particle tracking provide a 2D view of a

3D region of interest. For studies of 2D phenomena, such as colloidal motion in confined layers or transport in biological membranes, this limitation is acceptable. Indeed, 2D particle-tracking microscopy has enabled researchers to study the dynamics of diverse small objects ranging from microscale colloids to nanoscale molecular motor proteins.[1–3] However, the real world is 3D, and in many situations 2D measurements do not provide enough information. For instance, the interaction between a particle and a 2D patterned surface, as occurs in some directed self-assembly processes,[4–6] depends on the particle's motion normal to the surface (z) in addition to its trajectory relative to the lateral (xy) structure of the pattern. 2D information can also be difficult to interpret when analyzing the diffusion of objects that emit or scatter light anisotropically. Furthermore, the ability to localize a particle in three dimensions in real time will be required for feedback-controlled nanoparticle positioning and placement.[7,8]

In this article we introduce a fast, simple method for obtaining 3D particle trajectories directly from 2D digital video microscopy images. This method relies on microfabricated pyramidal wells whose faces are small mirrors oriented in such a way that multiple orthogonal views of the volume of interest are projected alongside the direct image. Substrates containing these pyramidal micromirror wells (PMWs) are used in a conventional microscope; the microscope is not otherwise altered, in contrast with other 3D microscopy strategies.[9,10] PMWs have recently been used to image biological cells in 3D from multiple perspectives and to track cell components,[11] and have also been used in on-chip magneto-optical traps for atom trapping and cooling.[12] Here we extend this technique to 3D nanoparticle tracking and present the first quantitative evaluation of the measurement precision. Our achieved measurement precision is < 20 nm in all three dimensions over 3 ms camera integration time and is limited by our signal-to-noise. When using an algorithm we recently developed, the image processing time is a fraction of the integration time, indicating that the technique could enable real-time 3D feedback control. However, while the measured *precision* is high, we also find some systematic errors which degrade the measurement *accuracy*. We argue that the errors arise from aberrations due to the geometrical placement of the mirrors rather than any imperfections in the mirrors themselves, and suggest strategies for overcoming them.

The orthogonal tracking principle is illustrated in Fig. 1a. When a particle moves parallel to the optical axis of the microscope, the direct image is stationary, but the point of reflection slides up and down the mirror; the reflected

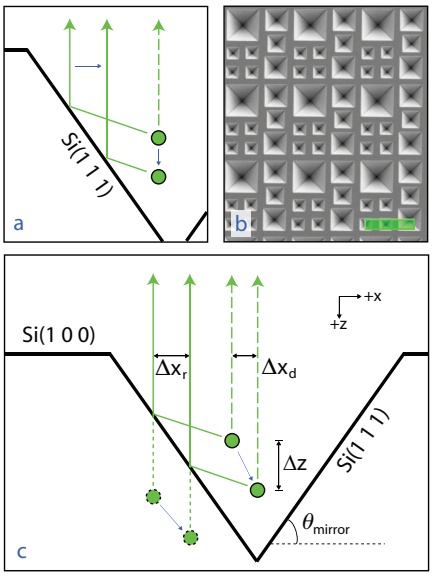

Figure 1: a) Orthogonal tracking principle. As a particle moves vertically in the well, the reflection slides along the sidewall mirror, converting the vertical particle motion to lateral image motion. The incident and reflected rays are not strictly perpendicular because the true sidewall angle is $\theta_{mirror} = 54.7°$. The reflections off the opposite sidewall have been omitted for clarity. b) SEM image of PMW sample. Scale bar is 50 μm. c) Expanded schematic diagram which illustrates the terms in Eq. 1. For $\theta_{mirror} \neq 45°$, the x and z axes are coupled. Note the longer focal depth of the reflected images.

image moves laterally in the xy plane. The vertical motion is converted to lateral motion relative to the camera, allowing us to use fast centroid-based image analysis (rather than nonlinear diffracted-ring fitting[13,14] or imprecise matching to a calculated pattern library[15,16]) to obtain the vertical as well as the lateral position of the particle. This arrangement also collects reflected light that would be missed under the conventional geometry; with perfectly reflecting mirrors, the information content can be increased up to fourfold, improving localization precision.[17] Furthermore, the fact that the vertical motion is projected into lateral motion means that, given sufficient reflectivity, the intrinsic z resolution is the same as that of x and y. For the same reason, an instrument carefully calibrated in the two lateral dimensions is in principle automatically calibrated in the third.

Results and Discussion

We fabricated PMWs in silicon substrates using standard photolithography and anisotropic wet etching (Fig. 1b; see Methods), and used them to perform orthogonal tracking experiments with fluorescent polystyrene beads of 190 nm diameter in a commercial epifluorescence microscope. Digital video sequences were processed using virtual window center-of-mass[8] (VWCM), a technique we recently developed. This centroid-based algorithm suppresses background contributions by iteratively truncating the region of interest so that the particle image is centered on it with subpixel precision. We used VWCM because it simplified our data analysis and because its speed makes it a candidate for real-time control applications. It is also robust against variations in the shape or size of the particle image,[8] a helpful feature when tracking particles in 3D with high-NA objectives. Where noted, for comparison with VWCM, we analyzed trajectories with Gaussian fitting, which yields the most precise measurements for well-focused spots but requires orders of magnitude more processing time.

Figure 2 is a series of frames from a standard CCD camera video sequence of an orthogonal tracking experiment (available online as Supporting Information). The particle is in the lower left corner of a well nominally 30 μm wide; reflected images appear on the left and lower faces. The microscope was approximately focused on the reflections, which appear as tight spots while the direct image appears as a ringed diffraction pattern. Because the reflected optical path is longer than the direct path, the focal plane is ≈ 5 μm beyond the z position of the particle in the well. The video shows that the reflections move in a fashion correlated with the direct image, and that the motion of the reflected spots along the line connecting them with the direct spot indicates the depth of the particle relative to the viewing plane. It is straightforward to compute the centroids of the three spots; once they are identified as containing XY, YZ and XZ information, those 2D trajectories can be immediately combined to yield a 3D trajectory (Fig. 3).

In the conversion from 2D to 3D, two trigonometric complications arise because θ_{mirror} is not the ideal angle of 45°. First, the different angle introduces a scaling factor in the conversion of vertical to lateral motion. Second, if $\theta_{mirror} \neq 45°$, the axes are coupled; the depth must be corrected for the distance between the direct and reflected images. Both effects can be compensated exactly by applying the law of reflection. For the geometry shown

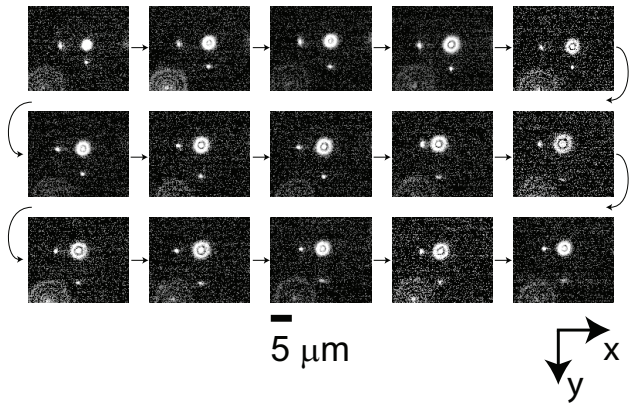

Figure 2: Series of images from orthogonal tracking movie of a 190 nm diameter particle in a water/glycerine solution. The frame rate was 59 frames per second, and the images displayed are at 30-frame (approximately half-second) intervals. Two reflections appear in the figure because the particle is in the lower left corner of a well. (The partial image in the lower left corner of each frame is of another particle outside the well, between the substrate and cover slip.)

in Fig. 1c we find (see Supporting Information for a more general form):

$$\Delta z = \Delta x_r \csc(2\theta_{mirror}) - \Delta x_d \cot(2\theta_{mirror}). \quad (1)$$

Here the subscripts r and d refer to the reflected and direct images respectively. Note that when $\theta_{mirror} = 45°$, $\Delta x_r = \Delta z$; note also that the uncoupled x motion can be obtained from a different orthogonal reflection rather than from the direct image, if desired.

The particle-mirror separation in our experiments is typically limited to distances $\gtrapprox 1$ μm and $\lessapprox 10$ μm for two reasons. First, in order to track particles without fitting, the separation between the direct and reflected images must be on the order of at least one wavelength. Second, the particle must also be close enough to the mirror that the difference in focus between the direct and reflected images is not so large that they overlap. We used a 40x "high-dry" objective because its numerical aperture (0.95) was lower than that of a 60x water-immersion objective (1.2), reducing the size of the direct diffracted ring so it did not overlap the reflections as frequently.

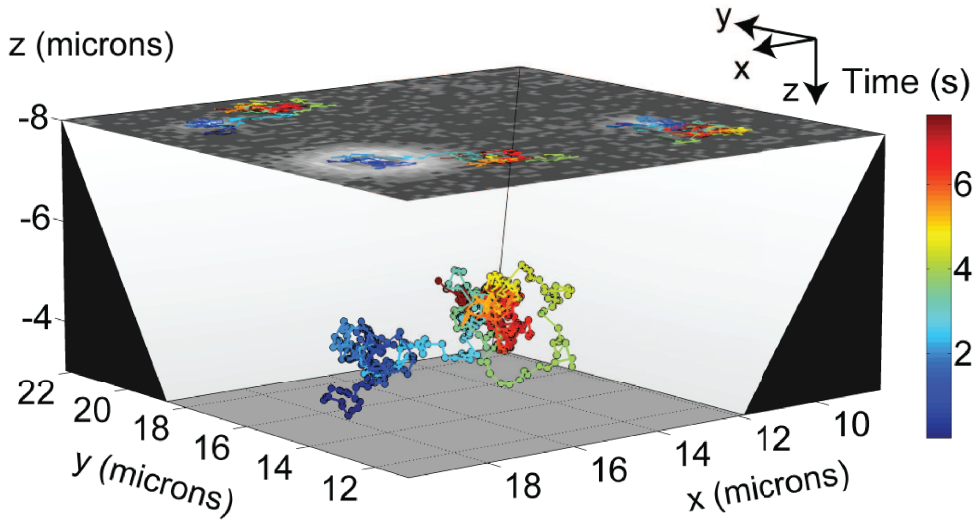

Figure 3: 3D trajectory formed by analysis of the movie represented by Fig. 2. The perspective is from the "northeast" corner of the frames in the movie. The top overlay image is a single frame (nonlinearly scaled for visibility) of the grayscale movie from which the trajectory was derived; the colored tracks on the overlay are the 2D tracks that result from processing the movie. The well walls have been drawn at approximately correct locations.

Orthogonal tracking permits particles whose direct images overlap to be easily distinguished by their different reflections. Fig. 4 depicts the simultaneously-obtained 3D trajectories of two particles vertically separated in a well. Although the direct images overlap (see inset), the particles are resolved and unambiguously identified by the common z motion of their reflections. Both trajectories are found without fitting. While the precision is diminished because the direct images are discarded, it is difficult to see how this task could be accomplished by other techniques.

All tracking methods are ultimately judged by their precision (the spread of estimated values in a measurement) and accuracy (the relation of the estimates to the correct value). We now consider these in turn, treating precision first. Ideally, we would estimate both localization precision and accuracy by repeatedly measuring the position of a particle fixed at a 3D location (*i.e.* with a nanopositioning stage) within a PMW; this method is unavailable to us because we require the particle to move relative to the sub-

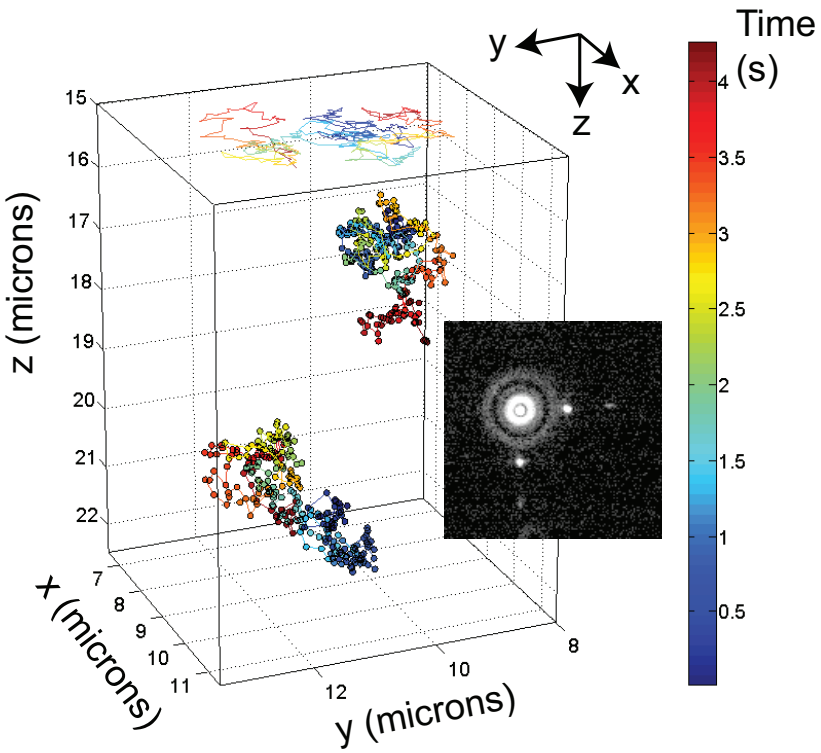

Figure 4: 3D trajectories of two overlapping particles by orthogonal tracking. Inset: Movie frame showing the overlap of the direct images of the particles and the well-resolved reflections. Movie is available as Supporting Information.

strate. However, it *is* possible to estimate the localization precision directly from the tracking data, by examining the average particle motion at different time intervals[18] (see Supporting Information). The ability to determine measurement precision in this way depends upon the time resolution; resolving smaller measurement noise requires the use of a smaller time step.

Precision. To test the precision, we captured a movie with a high-speed, high-sensitivity, low-noise EMCCD camera (see Supporting Information) of a particle diffusing in a water/glycerin mixture (glycerin volume fraction 80 %). The 3 ms frame duration was short enough to resolve measurement noise as small as 10 nm in 2D tests (data not shown). We analyzed the trajectory both with VWCM and with Gaussian fitting. We compared our results with

a rough theoretical estimate of the expected localization precision in Ref. [19, Eq. (17)]. (When combining the results of independent measurements to account for all available information, we weight the contributions of the independent measurements according to their respective variances. We quote the standard deviations obtained in this way.)

We found that both the Gaussian fit precision ($\sigma_x = 13$ nm; $\sigma_y = 16$ nm; $\sigma_z = 15$ nm) and the VWCM precision ($\sigma_x = 16$ nm; $\sigma_y = 19$ nm; $\sigma_z = 16$ nm) agree reasonably with the precision expected from the expression referenced above ($\sigma_{x,y,z} \approx 17$ nm). These results are not a fundamental precision limit by any means. We have used bare Si mirrors and standard cover glass; the signal-to-noise could be increased perhaps by using more reflective mirrors (*e.g.*, Al) or by using a fused silica cover glass. We have also chosen an unfavorable case with a badly defocused direct image. The precision in the central spot is ≈ 60 nm, contributing almost no improvement to the x and y estimates from the reflected spots. We note that the VWCM is two orders of magnitude faster than the Gaussian fit, even when only the in-focus reflections are analyzed in order to optimize the performance (and appropriateness) of Gaussian fitting. When the two well-focused spots were analyzed by VWCM the image processing time per frame was 0.5 ms, while the Gaussian fit time was 47 ms; with the defocused direct image included, the VWCM time per frame was still only 1.2 ms.

Accuracy. While the high precision we have demonstrated is desirable, it is no guarantee of overall accuracy. Because orthogonal tracking offers multiple independent measurements of each coordinate, we may compare those measurements to look for systematic errors. In particular, when we compare the two z-coordinate measurements from orthogonal faces, we find a systematic discrepancy between them which depends on the xy location of the particle - *i.e.*, the position of the particle relative to the micromirrors. The discrepancy can be as large as 100 nm in z over an xy travel of 500 nm (see Supporting Information). We have observed this bias in many different measurements of different samples, with different microscope objectives, and with different cameras. It appears with VWCM, Gaussian fitting, and the "Gaussian mask" algorithm.[19] As always, it is important to eliminate as many microscope aberrations as possible. We therefore took pains to optimize the cover-glass correction collar settings and to eliminate tilt ($< 0.05°$) of the cover glass relative to the focal plane of the objective,[20,21] or of the sample relative to the cover glass; the bias persists regardless.

Repeated observations and preliminary simulations strongly suggest that

this bias results from a kind of aberration unique to PMWs. This aberration stems simply from having an angled micromirror in the microscope field of view. The following factors contribute to the aberration. First and foremost, we have used high-NA objectives; if the objective collection angle is large compared with θ_{mirror}, the angular aperture of a reflected image is truncated asymmetrically. Second, the Fresnel reflection coefficients for a silicon/water interface depend strongly on angle, and with high-NA objectives the collected light experiences many reflected angles. (This effect could be avoided with aluminum mirrors, whose relative variation in Fresnel coefficients is much smaller.) Either of these effects alone could give rise to a shift or distortion of the image as the particle moves away from focus - hence, as the particle moves toward or away from the micromirrors. Furthermore, these effects could be exacerbated by spherical aberration, which is generally present when imaging through a water layer on the far side of a cover glass, and is worse for dry than for water-immersion objectives.

A complete optical analysis is beyond the scope of this article, but we can make some preliminary suggestions for mitigating the errors. The best results are usually obtained when the reflections are close to focus. If numerical aperture effects dominate, aberrations could be mitigated by 1) reducing the objective NA (of course, reducing the NA reduces light collection and hampers precision) or 2) making micromirrors at a shallower angle,[22] so that the micromirror "NA" exceeds the objective NA. It also remains possible (though perhaps undesirable) to calibrate for the bias; the discrepancy appears to be approximately linear in the lateral displacement. Furthermore, since orthogonal tracking is compatible with optical post-processing techniques such as multicolor imaging,[23] multifocal imaging[14] and wavefront coding,[24] techniques like the latter two that extend the effective focal depth could reduce systematic errors that worsen with defocus. We also note that the importance of the bias problem depends strongly on the application. For example, active feedback-controlled particle assembly applications will be limited primarily by precision constraints, not by the inherent accuracy of the technique. Thus, we believe that orthogonal tracking in conjunction with VWCM analysis is an excellent candidate for fast localization and feedback control of nanoparticles in 3D with nanometer precision.

Conclusion

We have demonstrated fast, high-resolution 3D particle tracking in PMWs. Because extra light is collected along different directions, the technique should provide 3D orientation information regarding asymmetric particles like rods or single quantum dots. PMW substrates can be mass-produced for biological[11] or nanofabrication applications. Truncated PMWs with a flat surface of silicon or glass (*i.e.* silicon-on-insulator) could be fabricated and patterned for exploring 3D particle-surface and particle-feature interactions. We have demonstrated 3D localization precision < 20 nm over 3 ms time intervals, with image processing time 1/3 of the frame time, indicating the possibility of real-time feedback-controlled assembly applications.

Methods

To fabricate microscopic angled mirrors, we modified silicon substrates as follows. Silicon wafers were coated with a silicon nitride layer 80 nm thick by low-pressure chemical vapor deposition. A polymer resist layer was spun onto the wafer, selectively exposed to UV light through a chrome photomask, and developed to remove exposed resist. Reactive ion etching was used to remove exposed nitride. The Si substrate was anisotropically etched in a hot aqueous KOH bath (80 °C, KOH volume fraction 45 %) for $\approx$ 1 hr to the maximum depth, yielding PMWs with four faces intersecting in a point at the bottom (Fig. 1b). The etch stop for KOH is the Si (1 1 1) crystal plane, whose angle relative to the (1 0 0) surface plane is $\theta_{mirror} = 54.7°$. (The ratio of etch rates between (1 0 0) and (1 1 1) planes is ≈ 600.[25]) Substrates were subsequently bathed in dilute hydrochloric acid to remove contaminant particles[26] and etched in dilute hydrofluoric acid to remove the nitride layer. This procedure yielded a sufficiently smooth, mirror-like surface on the etched walls.

Suspensions of fluorescent-dyed (480 nm excitation/520 nm emission wavelength) polystyrene spheres of 190 nm diameter in water (with trace amounts of surfactant) were diluted with water and glycerin (glycerin volume fraction $\approx$ 40 % except where noted) to particle concentrations $\approx 10^{10}$ cm^{-3}. Small volumes ($\approx$ 1.5 μL) of this solution were pipetted on these substrates and covered with a cover glass 170 μm thick for viewing with a commercial inverted epifluorescence microscope. We estimate the liquid layer thickness

between the cover glass and substrate as $\leq$ 2 μm. Fluorescence was excited in the microscope with a 488 nm solid-state laser. Emitted fluorescence was collected with a plan apochromat objective (40x/0.95 NA) through a dichroic mirror and an emission bandpass filter, and was recorded either directly with a standard 8-bit charge-coupled device (CCD) video camera having 60 s^{-1} maximum frame rate and pixel width 7.4 μm, or through an additional 2x magnification lens with a Peltier-cooled, back-thinned, 16-bit electron-multiplication charge-coupled device (EMCCD) video camera having 500 s^{-1} maximum frame rate, pixel width 24 μm, and quantum efficiency $\approx$ 90 % over the emission spectrum of the fluorescent beads.

Acknowledgements. This research was performed at the NIST Center for Nanoscale Science and Technology. AJB was supported by the National Research Council. The authors thank G. Stein and the CNST NanoFab staff for fabrication advice and assistance, and S. Stavis and L. Whitman for helpful discussions.

Supporting Information Available: Movies of orthogonal tracking experiments and a derivation of the error analysis with corroborating figures. This material is available free of charge via the Internet at http://pubs.acs.org.

References

1. Crocker, J. C.; Grier, D. G. Microscopic Measurement of the Pair Interaction Potential of Charge-Stabilized Colloid. *Phys. Rev. Lett.* **1994**, *73*, 352–355.

2. Sainis, S. K.; Germain, V.; Dufresne, E. R. Statistics of Particle Trajectories at Short Time Intervals Reveal fN-Scale Colloidal Forces. *Phys. Rev. Lett.* **2007**, *99*, 018303.

3. Yildiz, A.; Forkey, J. N.; McKinney, S. A.; Ha, T.; Goodman, Y. E.; Selvin, P. R. Myosin V Walks Hand-Over-Hand: Single Fluorophore Imaging with 1.5-nm Localization. *Science* **2003**, *300*, 2061–2065.

4. Kraus, T.; Malaquin, L.; Schmid, H.; Riess, W.; Spencer, N. D.; Wolf, H. Nanoparticle Printing with Single-Particle Resolution. *Nature Nano.*, **2007**, *2*, 570–576.

5. Cheng, W.; Park, N.; Walter, M. T.; Hartman, M. R.; Luo, D. Nanopatterning Self-Assembled Nanoparticle Superlattices by Moulding Microdroplets. *Nature Nano.*, **2008**, *3*, 682–690.

6. Zhang, Q.; Dang, C.; Urabe, H.; Wang, J.; Sun, S.; Nurmikko, A. Large Ordered Arrays of Single Photon Sources Based on II-VI Semiconductor Colloidal Quantum Dot. *Opt. Express*, **2008**, *16*, 19592–19599.

7. Armani, M.; Chaudhary, S.; Probst, R.; Shapiro, B. Using Feedback Control and Micro-Fluidics to Independently Steer Multiple Particles. *IEEE J. Microelectromech. Syst.* **2006**, *15*, 945–956.

8. Berglund, A. J.; McMahon, M. D.; McClelland, J. J; Liddle, J. A. Fast, Bias-Free Algorithm for Tracking Single Particles with Variable Size and Shape. *Opt. Express* **2008**, *16*, 14064–14075.

9. Prasad, V.; Semwogerere, D.; Weeks, E. R. Confocal Microscopy of Colloids. *J. Phys.: Condens. Matter* **2007**, *19*, 113102.

10. Wu, H.-J.; Everett, W.; Anekal, S.; Bevan, M. Mapping Patterned Potential Energy Landscapes with Diffusing Colloidal Probes. *Langmuir* **2006**, *22*, 6826–6836.

11. Seale, K. T.; Reiserer, R. S.; Markov, D. A.; Ges, I. A.; Wright, C.; Janetopoulos, C.; Wikswo, J. P. Mirrored Pyramidal Wells for Simultaneous Multiple Vantage Point Microscopy*J. Microsc.* **2008**, *232*, 1–6.

12. Trupke, M.; Ramirez-Martinez, F.; Curtis, E. A.; Ashmore, J. P.; Eriksson, S.; Hinds, E.A.; Moktadir, Z.; Gollasch, C.; Kraft, M.; Prakash, G. V.; et al. Pyramidal Micromirrors for Microsystems and Atom Chips. *Appl. Phys. Lett.* **2006**, *88*, 071116.

13. Speidel, M.; Jonáš, A.; Florin, E. L. Three-Dimensional Tracking of Fluorescent Nanoparticles with Subnanometer Precision by Use of Off-Focus Imaging. *Opt. Lett.* **2003**, 28, 69–71.

14. Toprak, E.; Balci, H.; Blehm, B. H.; Selvin, P. R. Three-dimensional Particle Tracking Via Bifocal Imaging. *Nano Lett.* **2007**, *7*, 2043–2045.

15. Park, J. S.; Choi, C. K.; Kihm, K. D. Temperature Measurement for a nanoparticle Suspension by Detecting the Brownian Motion Using Optical Serial Sectioning Microscopy (OSSM).*Meas. Sci. Technol.* **2005**, *16*, 1418–1429.

16. Luo, R.; Yang, X. Y.; Peng, X. F.; Sun, Y. F. Three-dimensional Tracking of Fluorescent Particles Applied to Micro-Fluidic Measurements. *J. Micromech. Microeng.* **2006**, *16*, 1689–1699.

17. Ober, R. J.; Ram, S.; Ward, E. S. Localization Accuracy in Single-Molecule Microscopy. *Biophys. J.* **2004**, *86*, 1185–1200.

18. Savin, T.; Doyle, P. S. Static and Dynamic Errors in Particle Tracking Microrheology. *Biophys. J.* **2005**, *88*, 623–638.

19. Thompson, R.; Larson, D; Webb, W. *Biophys. J.* Precise Nanometer Localization Analysis for Individual Fluorescent Probes. **2002**, *82*, 2775–2783.

20. Arimoto, R.; Murray, J. M. A Common Aberration with Water-Immersion Objective Lenses. *J. Microsc.* **2004**, *216*, 49–51.

21. Sluder, G.; Wolf, D. E., eds. *Digital Microscopy*; Academic Press: Amsterdam, 2007.

22. Resnik, D.; Vrtacnik, D.; Aljancic, U.; Mozek, M.; Amon, S. The Role of Triton Surfactant in Anisotropic Etching of 1 1 0 Reflective Planes on (1 0 0) Silicon. *J. Micromech. Microeng.* **2005**, *15*, 1174–1183, and references therein.

23. Bausch, A. R.; Weitz, D. A. Tracking the Dynamics of Single Quantum Dots: Beating the Optical Resolution Twice. *J. Nanoparticle Res.* **2002**, *4*, 477–481.

24. Cathey, W. T.; Dowski, E. R. New Paradigm for Imaging Systems. *Appl. Opt.* **2002**, *49*, 6080–6092.

25. Madou, M. J. *Fundamentals of Microfabrication*; CRC Press: Boca Raton, Florida, 1997; p. 171.

26. Nielsen, C. B.; Christensen, C.; Pedersen, C.; Thomsen, E. V. Particle Precipitation in Connection with KOH Etching of Silicon. *J. Electrochem. Soc.* **2004**, *151*, G338-G342.